



Lidar temperature series in the middle atmosphere as a reference data set. Part B: Assessment of temperature observations from MLS/Aura and SABER/TIMED satellites

Robin Wing¹, Alain Hauchecorne¹, Philippe Keckhut¹, Sophie Godin-Beekmann¹, Sergey Khaykin¹, and Emily M. McCullough²

¹LATMOS/IPSL, UVSQ Université Paris-Saclay, Sorbonne Université, CNRS, Guyancourt, France

²Department of Physics and Atmospheric Science, Dalhousie University, Halifax, Canada

Correspondence to: Robin Wing (robin.wing@latmos.ipsl.fr)

Abstract. We have compared 1338 nights of Rayleigh lidar temperatures measured at L'Observatoire de Haute Provence (OHP) with co-located temperature measurements from the Microwave Limb Sounder (MLS) and the Sounding of the Atmosphere by Broadband Emission Radiometry instrument (SABER). The comparisons were conducted using data from January 2002 to January 2011 in the geographic region around the observatory (43.93° N, 5.71° E). We have found systematic differences between the temperatures measured from the ground based lidar and those measured from the satellites which suggest non-linear distortions in the satellite altitude retrievals. We see a winter stratopause cold bias in the satellite measurements with respect to the lidar (-6 K for SABER and -15 K for MLS), a summer mesospheric warm bias (10 K near 60 km), and a vertically structured bias for MLS (0 to 4 K). We have corrected the stratopause height of the satellite measurements using the lidar temperatures and have seen an improvement in the comparison. The winter stratospheric relative cold bias between the lidar and SABER has been eliminated and the summer mesospheric warm bias is reduced by 6 K. Stratopause altitude corrections have reduced the relative cold bias between the lidar and MLS by 4 K in the early autumn and late spring.

1 Introduction

Satellite atmospheric measurements are vital for providing global assessments of long term atmospheric temperature trends. However, particular care must be taken to validate each new satellite as well as provide periodic ground checks for the entire instrument lifetime in order to counter drifts in calibration and local measurement time (Wuebbles et al., 2016). Changes in satellite measurements



20 can occur over the course of a mission due to instrument degradation, calibration uncertainties, orbit
changes, and errors/assumptions in the forward model parameters. Additionally, most mission plan-
ning agencies have guidelines which require that satellite programs conduct formal validation studies
to ensure accuracy and stability of the measurements (Council, 2007). In this work we will show the
value of our improved Rayleigh lidar temperature profiles, described in (Wing et al., 2018a), as a
25 validation tool in the middle atmosphere .

In this work we briefly outline some alternative remote sensing and in situ techniques for mea-
suring temperature in the middle atmosphere and state the strengths and weaknesses of these mea-
surements with respect to a lidar measurement Sect. 1.1. In Sect. 1.2 we outline several previous
lidar-satellite temperature comparison studies and contrast their methods to our study. Following the
30 introduction is a brief description of the instruments involved in the study (Sect. 2), a definition of the
geographic area under consideration, and several criteria for determining coincidence between lidar
and satellite measurement profiles (Sect. 3). In Sect. 4 we directly compare temperature profiles from
MLS and SABER to the lidar temperatures and show a monthly median difference climatology and
note several systematic differences. Section 5 details a procedure to correct the satellite temperature
35 profiles based on the height of the stratopause in the lidar data. Finally, Sect. 6 shows an improved
lidar-satellite monthly median difference climatology based on the altitude corrected satellite data.

1.1 Alternative Measurement Techniques

Rayleigh lidar remote sounding of atmospheric density and temperature is an excellent tool for use
in validating satellite measurements over a specified geographic area and vertical range. Lidars can
40 make accurate and high resolution measurements over a large portion of the middle atmosphere; in
regions which are notoriously difficult for other techniques to measure routinely or precisely. There
are three key strengths in the Rayleigh lidar technique which set it apart from other atmospheric
sounders. First is the ability to retrieve an absolute temperature profile from a measured relative
density profile with very high spatio-temporal accuracy and precision. Second, the vertical error and
45 resolution of a lidar measurement is constant with altitude which allows us to sample the upper
middle atmosphere with the same range resolved confidence as the lower middle atmosphere and
troposphere. Third, raw lidar measurements don't suffer from vertical distortion in the altitude vector
- that is to say that there is insignificant kernel overlap between adjacent measurement elements in
space or time.

50 Other current measurement techniques for this region of the atmosphere include:

a) Rocketsondes were used during the early satellite era to make in situ measurements of the
middle atmosphere but this technique has many well known limitations and requires large corrections
and uncertainties in the upper mesosphere (Johnson and Gelman, 1985).



b) Meteor radar techniques provide an estimation of the temperature at 90 km and can operate
55 on a near continuous basis but they require several a priori assumptions and must be calibrated with
data from an independent source (Meek et al., 2013)

c) Satellites, like MLS (Microwave Limb Scanner) and SABER (Sounding of the Atmosphere by
Broadband Emission Radiometry), provide globally distributed temperature measurements at sev-
eral pressure levels throughout the vertical atmospheric column (Waters et al., 2006) (Mertens et al.,
60 2001). Satellite based measurements provide a very good global view of the Earth's middle atmo-
sphere but can suffer from calibration errors, temporal coverage gaps, and problems with vertical
resolution.

d) OH airglow imagers (Pautet et al., 2014) which provide high spatio-temporal resolution 2D
images of temperature perturbations derived from OH emissions near 87 km

65 Considered together, this suite of remote sensing techniques can provide a comprehensive view of
the middle atmosphere. The inclusion of Rayleigh lidar data into multi-sensor studies of the middle
atmosphere provides an important local ground truthing perspective which helps to refine the global
view offered by other techniques.

1.2 Previous Lidar-Satellite Temperature Studies

70 Previous studies comparing ground based lidar and satellite measurements of temperature have often
used Sodium Resonance lidars to compare the lidar derived neutral temperature between 85 km and
105 km to satellite temperatures in the mesopause region. Studies of this sort have generally shown
good agreement between ground and satellite observations (Xu et al., 2006). Due to the strength of
Na lidars in the upper mesosphere they naturally lend themselves well to studies of tides and wave
75 breaking dynamics. A study by (Yuan et al., 2010) compared Na lidar and SABER temperatures in
the context of a 6 year tidal analysis. They found semiannual disagreements in the tidal amplitude
around the spring and autumn equinoxes with a maximum difference of 12 K near 90 km occurring in
February. Several explanations and partial corrections were offered but the phenomenon is robust and
the authors concluded that further study was required to fully resolve the temperature discrepancy.

80 Studies have also been done comparing temperatures calculated from the Rayleigh lidar tech-
nique and those derived from SABER and MLS observations. (Taori et al., 2011, 2012; Taori et al.,
2012) comprise an excellence series of publications using multiple instruments to measure the atmo-
spheric temperature from 40 km to 100 km. These works found good agreement between the lidar
and SABER up to 65 km and significant initialization errors in the lidar of up to 25 K near 90 km.
85 We have partially accounted for this initialization induced lidar warm bias in the companion paper
(Wing et al., 2018a). Our work here offers two improvements on these three publications. Firstly,
we have not focused as much on case studies but rather on the statistics of nearly a decade of lidar-
satellite inter-comparisons. Secondly, we have conducted our comparisons on a 1 km grid in an effort
to match small scale features in the temperature profiles.



90 A good lidar to satellite temperature comparison was done by (Siva Kumar et al., 2003) using
240 nights of lidar temperatures, temperatures from UARS, and model temperatures from CIRA-
86 and MSIS-90. They compared monthly and seasonal averages and found significant semiannual
temperature anomalies in the region of 45 – 50 km] in February-March and September-October as
well as initialization problems above 70 km. A second study by the same author compared 14 years of
95 monthly average lidar temperatures to temperatures from the satellites SABER, HALOE, COSMIC,
and CHAMP (Sivakumar et al., 2011). As with the previous study temperature anomalies of 3-
5 K were identified in the region near the stratopause. The differences were attributed to monthly
averaging and slight differences in measurement time and location of the lidar and satellites. The
approach employed in our work is to make comparisons of nightly averages and then study the
100 monthly median of the temperature differences – an approach which will allow for finer temporal
precision.

Another study which compares 120 nights of Rayleigh lidar temperatures measured over Beijing
to temperatures from SABER over the course of one year found good agreement between monthly
average temperature profiles (Yue et al., 2014). This study found winter time temperature anomalies
105 in the stratopause region and attempted to account for these features by fitting an annual, semi-
annual, and 3 month sinusoid to the data. The objective of our study is similar to that of Yue et al.
(2014) insofar as we are interested in the time evolution of lidar-satellite temperature comparisons
and identifying potential seasonal or decadal trends. However, we are seeking to make nightly tem-
perature comparisons between lidar and two satellites, SABER and MLS, over multiple years with-
110 out assuming large contributions from an Annual Oscillation (AO) or its harmonics. Our study uses
more than 5 times as many nights and spans over 8 times as long as the study in (Yue et al., 2014).

Further study of seasonal temperature anomalies between ground based lidar and SABER was
done by (Dou et al., 2009) comparing 2332 nights of lidar data from 6 different sites in the Network
for the Detection of Composition Change (NDACC) to zonally averaged temperature profiles from
115 SABER. This study found a 2-5 K systematic bias in the stratopause region and concluded that this
result may be due to either a bias in SABER, tidal aliasing, or sporadic aerosols. As well the study
found a systematic difference in the upper mesosphere attributed to tidal aliasing, bias in SABER
or AO. In our work we use a smaller geographic window and not a zonal average temperature to
compare more truly co-incident measurements. As well we limit the time difference between the
120 lidar and satellite measurements to minimize possible tidal contributions.

2 Instrumentation

The Observatoire de Haute Provence (OHP) Rayleigh lidar has been in operation in southern France
since 1978, making measurements of the upper stratosphere and lower mesosphere at 532 nm with a



maximum resolution of 2.4 min and 150 m. The details of the Rayleigh lidar algorithm and the OHP
 125 lidar specifications are presented in the companion publication (Wing et al., 2018a).

SABER is an broadband radiometer aboard NASA's TIMED (Thermosphere Ionosphere Meso-
 sphere Energetics Dynamics) satellite and makes temperature measurements based on CO₂ limb
 radiances from 20 km to 120 km. SABER has a vertical resolution of 2 km and random temperature
 errors of less than 0.5 K below 55 km, 1 K at 70 km, and 5 K at 100 km (Remsburg et al., 2008).
 130 TIMED does not have a sun synchronous orbit and does not pass through our OHP comparison area
 at a fixed local time. This makes finding temporally coincident measurements with the lidar rela-
 tively easy. We are using version 2.0 of the published SABER temperatures. Further information for
 SABER/TIMED can be found in (Mertens et al., 2001).

MLS is an microwave spectrometer aboard the Aura satellite and makes temperature measure-
 135 ments based on emissions from O₂ further information can be found in (Waters et al., 2006). MLS
 vertical averaging kernels have a full-width-half maximum of 8 km at 30 km, 9 km at 45 km, and
 14 km, at 80 km and a temperature resolution which goes from 1.4 K near 30 km to 3.5 K above
 80 km (Schwartz et al., 2008). We are using version 4.0 of the published MLS temperatures. MLS is
 a sun synchronous satellite which passes the equator around 1h45 UTC and is generally temporally
 140 coincident with the last hour or so of lidar measurements.

3 Comparison Parameters

Defining coincident measurements between satellites and lidars can be difficult due to temporal
 and spatial offsets, differences in viewing geometry, and different approaches to smoothing. Other
 studies such as García-Comas et al. (2014) have defined short time windows over a 1000 km square
 145 surrounding the observatory as sufficient for coincidence while others such as (Yue et al., 2014) have
 chosen to approach the problem by looking at monthly averages over a much narrower latitude band.

For this study we wanted to compare to satellite profiles geographically near the lidar to minimize
 latitudinal variations in the temperature and within a small time frame to minimize the contribution
 of tides, tidal harmonics, and gravity wave effects. This desire for close spatio-temporal matching
 150 was balanced against the need for a sufficiently large number of comparisons as to produce results
 which are statistically significant and useful. Ultimately, we decided on a geographic window of
 $\pm 4^\circ$ latitude and $\pm 15^\circ$ longitude similar to the analysis done by (Dou et al., 2009). We reasoned that
 the UMLT (Upper Mesosphere and Lower Thermosphere) structure would vary with latitude to a
 greater degree than with longitude and that the longitudinal separation between consecutive SABER
 155 satellite passes gives a natural bound on the longitude. Figure 1 shows the geographic extent of our
 study.

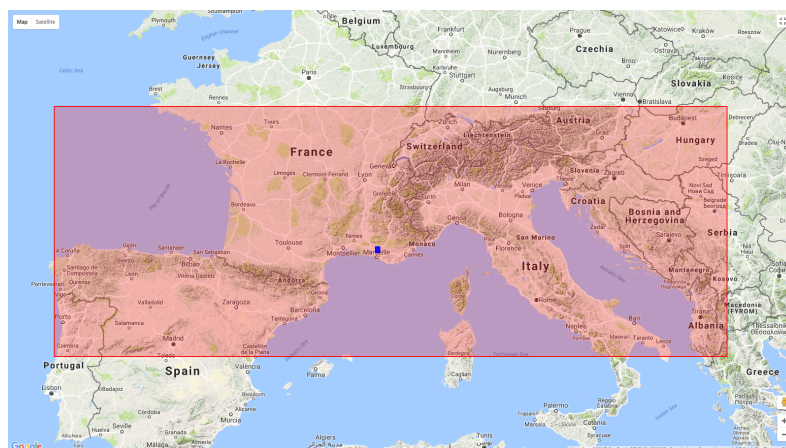


Figure 1: Area defined for coincident measurements (40° N, 35° E) to (48° N, 21° E). L'Observatoire de Haute-Provence in blue at (43.93° N, 5.71° E). (data: Google, 2017)

The minimum length of an OHP nightly lidar temperature measurement is four hours. We chose to use a ± 4 h window around the lidar measurement as the temporal limit for coincidence with a satellite pass. This gives us a roughly 12 h window centered around the middle of the lidar measurement.

Our choice was influenced by a desire to minimize the effect of the 12 h tidal harmonic. Previous work comparing between satellites have been able to take advantage of daytime satellite overpasses and chose to work within a ± 2 h window (Hoppel et al., 2008). (French and Mulligan, 2010) conducted a comparison between an OH spectrometer (in conjunction with a sodium lidar) and SABER at ± 15 min and ± 8 h and found no significant difference. However, it must be noted that this study was conducted at a latitude of 69° S and the comparison may not hold in the mid-latitudes.

4 Temperature comparisons without considering vertical offset

Here we demonstrate the directly-calculated temperature biases between OHP and both SABER and MLS which are present before we carry out the adjustment for satellite altitude offsets which are discussed in Sect. 5.

4.1 Comparison OHP Lidar and SABER

From 2002 to 2011 there were 621 coincident measurements of sufficient quality between OHP lidar and SABER. Figure 2 (upper panel) shows the monthly median temperature differences between the lidar and SABER while Fig. 2 (lower panel) shows the mean seasonal temperature bias with altitude.

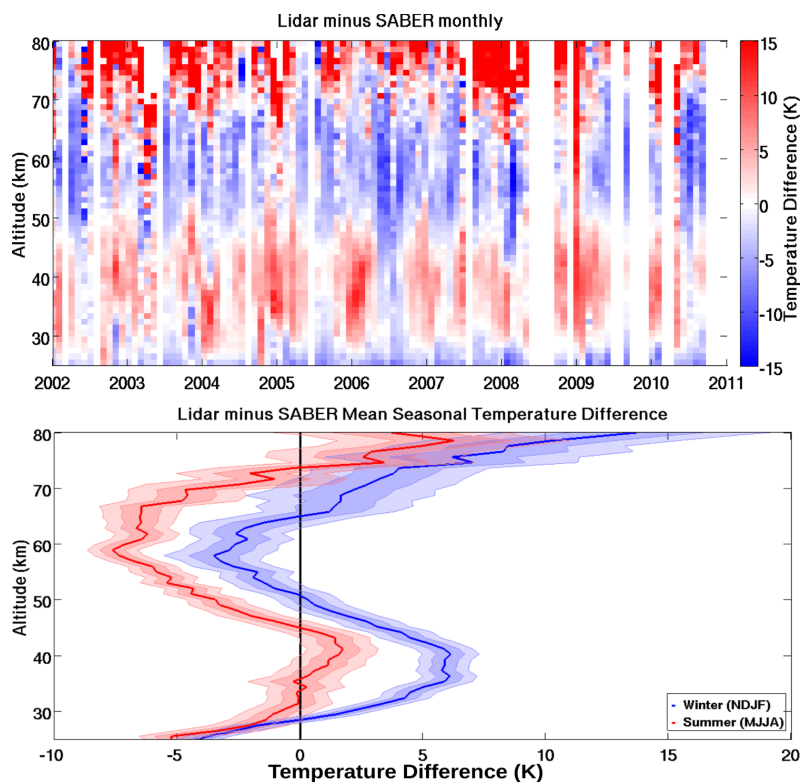


Figure 2: Nine year systematic comparison of OHP lidar and SABER temperatures. The monthly median temperature differences between the lidar and SABER are shown in the upper panel. Red indicates that the lidar is warmer than SABER and blue that the lidar is colder. There are 621 nights of coincident measurements in the colour plot. The lower panel is a seasonal ensemble of lidar minus SABER temperature differences. The summer (May, June, July, August) ensemble in red includes 174 nights of coincident measurements and the winter (November, December, January, February) ensemble in blue includes 221 nights of coincident measurements. Shaded errors represent 1 and 2 standard deviations.

The upper panel shows a relative warm bias for the lidar with respect to SABER above 70 km. Discrepancies in this region are likely due to lidar initialization errors and background uncertainty which we have attempted to minimize in the companion publication (Wing et al., 2018a). There is also an evident seasonal relative warm bias in the winter stratosphere between 35 km and 50 km - a region where lidar measurements are exceptionally accurate. The right hand panel shows a very distinctive ‘S’ shape to the bias in both the winter and summer ensembles which is indicative of a vertical offset between the lidar and satellite measurements. The basic ‘S’ shape bias was identified in studies of synthetic lidar data as being due to vertical offsets between lidar instruments (Leblanc



et al., 1998). Unfortunately, this offset is neither constant from night-to-night, nor constant with altitude as evidenced by the elongated and distorted nature of the ‘S’ shape.

If we bin all the temperature differences by month we can clearly see that there is a winter strato-
spheric warm bias near 40 km and a pronounced summer cold bias in the mesosphere near 60 km, as
shown in Fig. 3.

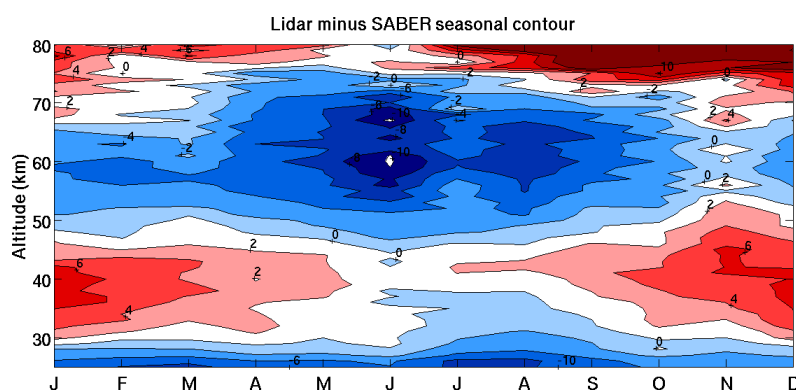


Figure 3: Monthly median temperature difference between lidar and SABER temperature measurements. Red indicates regions where the lidar measures warmer temperatures than SABER and blue regions where the lidar measures colder temperatures than SABER.

4.2 Comparison OHP lidar and MLS

From 2004 to 2011 there were 717 coincident measurements of sufficient quality between OHP lidar
and MLS. Figure 4 (upper panel) shows the monthly median temperature differences between the
lidar and MLS while Fig. 4 (lower panel) shows the mean seasonal temperature bias with altitude.

As was the case with the lidar-SABER comparison, in the upper panel we see a lidar warm bias
above 70 km and a strong winter stratospheric warm bias near 40 km. In this comparison the strato-
spheric warm bias appears to have a downward phase migration as the winter progresses. In the
corresponding lower panel we see very pronounced summer time systematic differences which al-
ternate from warm to cold throughout the stratosphere and mesosphere. The winter ensemble shows
a very large lidar warm bias near the stratopause.

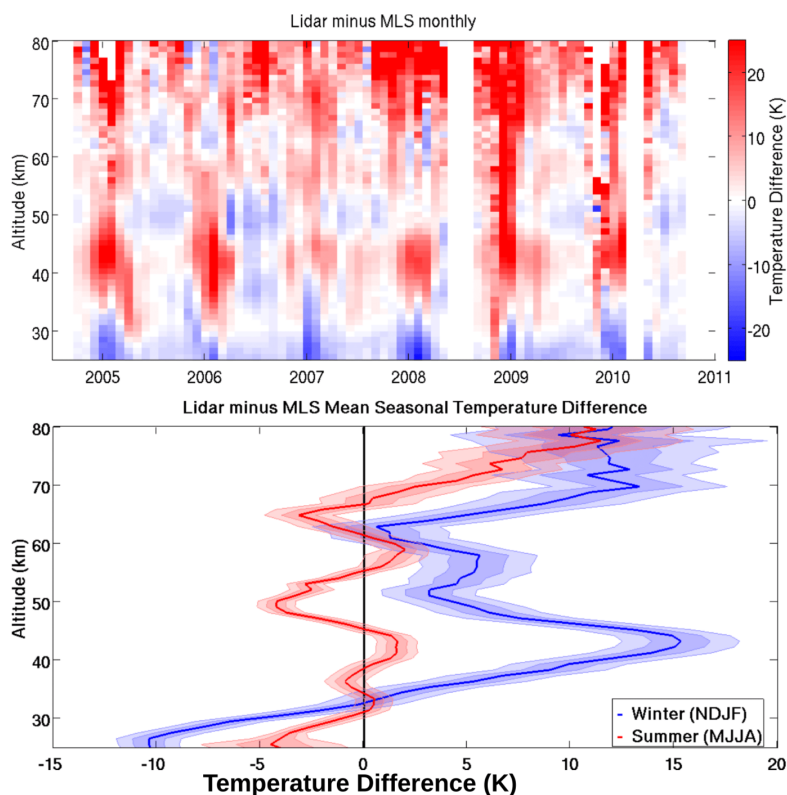


Figure 4: Six year systematic comparison of OHP lidar and MLS temperatures. The monthly median temperature differences between the lidar and MLS are shown in the upper panel. There are 717 nights of coincident measurements. The lower panel is a seasonal ensemble of lidar minus MLS temperature differences. The summer (May, June, July, August) ensemble in red includes 224 nights of coincident measurements and the winter (November, December, January, February) ensemble in red includes 269 nights of coincident measurements. Shaded errors represent 1 and 2 standard deviations.

Following the same procedure of binning lidar-MLS temperature differences by month we see a very pronounced downward phase progression of the winter stratospheric warm bias near 40 km. Additionally, there is an evident layered cold bias in the summer stratosphere and mesosphere. The three layers appear near 37 km, 50 km, and 65 km.

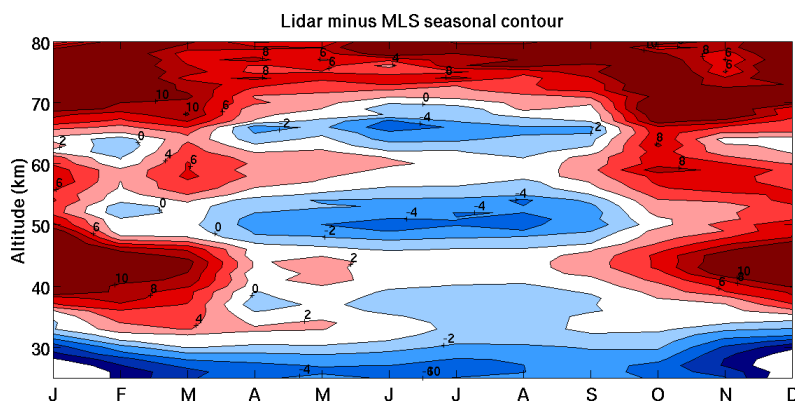


Figure 5: Monthly median temperature difference between lidar and MLS temperature measurements. Red indicates regions where the lidar measures warmer temperatures than MLS and blue regions where the lidar measures colder temperatures than MLS.

5 Minimizing Temperature Difference Between Lidar and Satellites with a Vertical Offset

We investigated a possible vertical offset between the lidar and satellite measurements to determine whether this could be contributing to the temperature biases seen in Sect. 4.

5.1 Method to determine the vertical offset between measurements

205 To match the two temperature profiles exactly in amplitude and altitude requires a unique altitude dependent correction factor for each comparison. However, we can make a rough estimate of the average vertical offset between the two measurements by focusing on the region of the stratopause which generally has a defined altitude and a clear structure. We used a simple least squares method to best estimate the vertical offset that would minimize the temperature differences between the lidar
 210 measurement and the satellite measurement. Two examples of this offset calculation for SABER are shown in Fig. 6 and two examples for MLS are shown in Fig. 7. the examples in these figures show nights where the lidar and satellite temperatures are in good agreement or can be brought into good agreement by applying a small vertical displacement. However, it is important to note that there are examples of lidar-satellite temperature measurements which cannot be brought into good agreement
 215 with small vertical displacements. Two such examples can be found in Fig. 8. These examples of poor agreement are almost exclusively found in winter on nights where the stratopause is greatly disturbed.

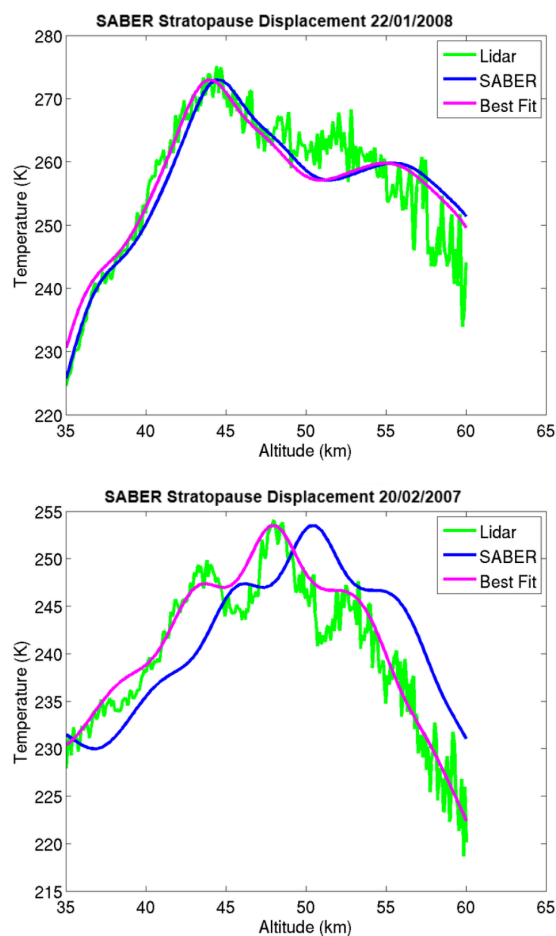


Figure 6: The upper panel shows a case where the lidar and SABER were well aligned in altitude. The lower panel shows a case where a vertical displacement of the SABER profile ameliorated the agreement with the lidar measurement.

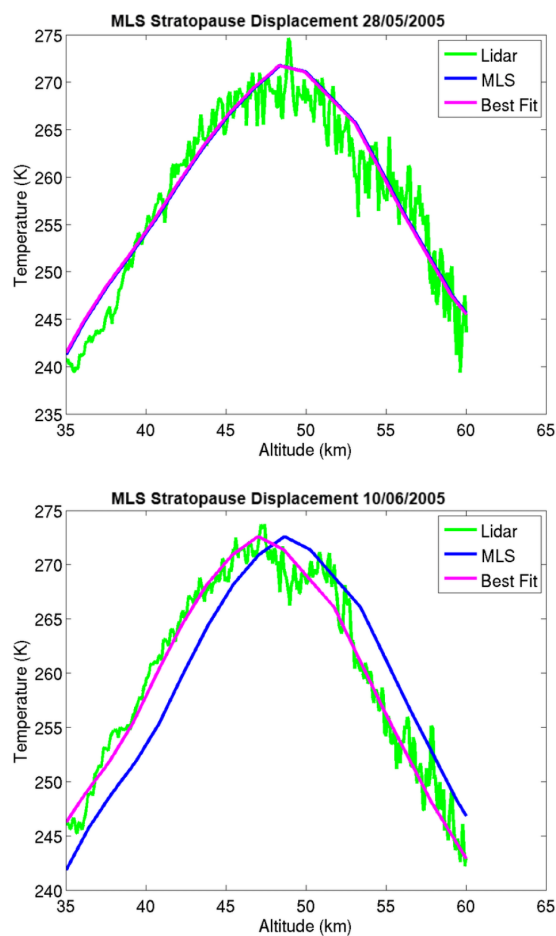


Figure 7: The upper panel shows a case where the lidar and MLS were well aligned in altitude. The lower panel shows a case where a vertical displacement of the MLS profile ameliorated the agreement with the lidar measurement.

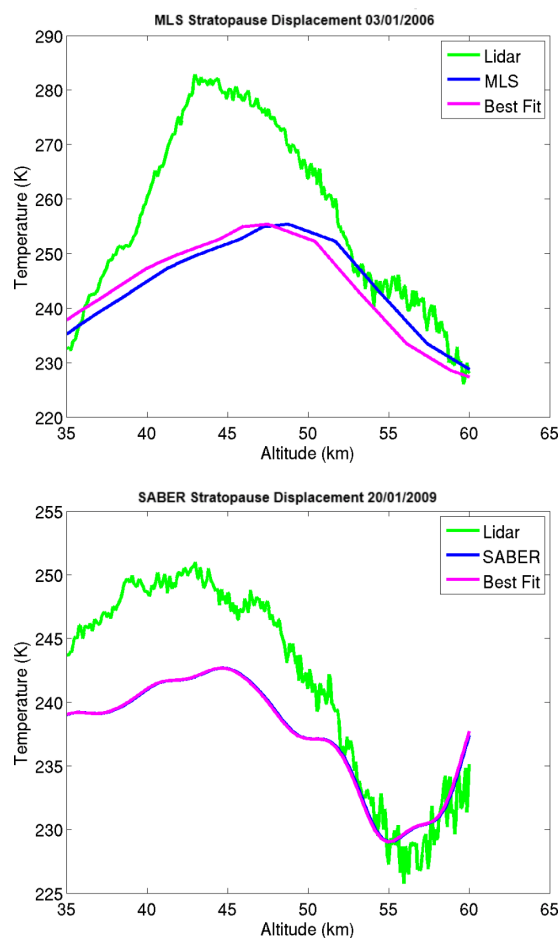


Figure 8: Two examples of poor matches between lidar and satellite temperature profiles (MLS upper panel, SABER lower panel). These mismatches mainly occur between late November and early April on nights where the stratosphere was disturbed and experiencing a warming.

5.2 Trends in Vertical Offset between Lidar and Satellites

We calculated an offset for every coincident measurement between the lidar and SABER and the
 220 lidar and MLS. The monthly average of this altitude offset value is represented in Fig. 9 as a black
 line with an associated standard deviation in grey. There is a clear, but imperfect, seasonality to this
 altitude displacement.

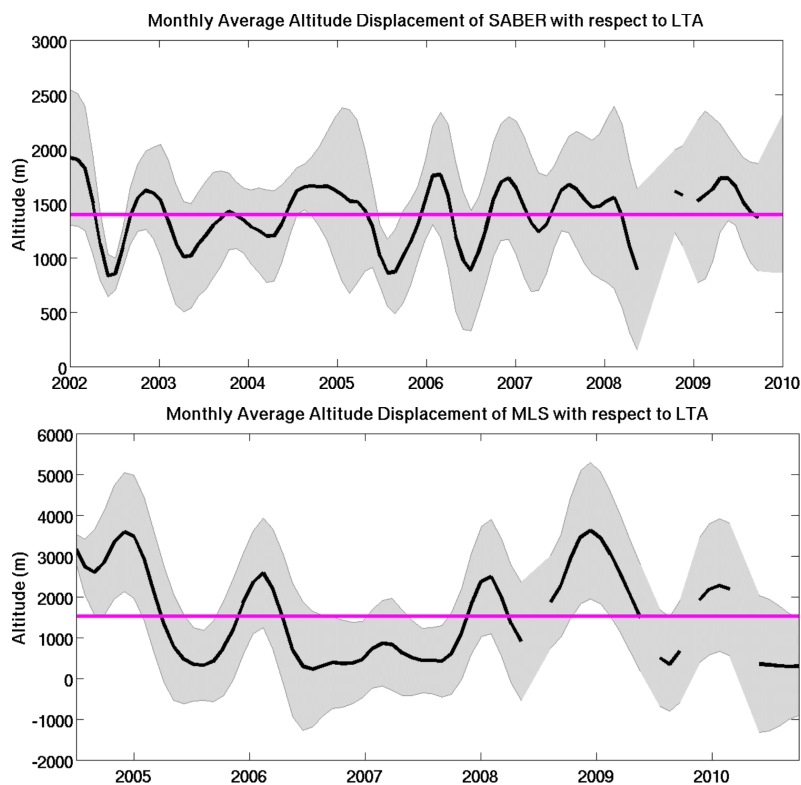


Figure 9: The upper panel features the monthly average displacement of SABER measurements with respect to the OHP lidar (black). The standard deviation is given as the shaded grey area. The mean offset (magenta) is 1425 m with a standard deviation of 262 m. The lower panel shows the same analysis with the monthly average MLS displacement. The mean value is 1738 m with a standard deviation of 1260 m.

Superimposing the traces shown in Fig. 9 onto the colour plots in Fig. 2 and Fig. 4 shows a clear correlation between lidar-satellite temperature anomalies and mean monthly altitude displacement
 225 between the lidar and satellite temperature profiles, as shown in Fig. 10.

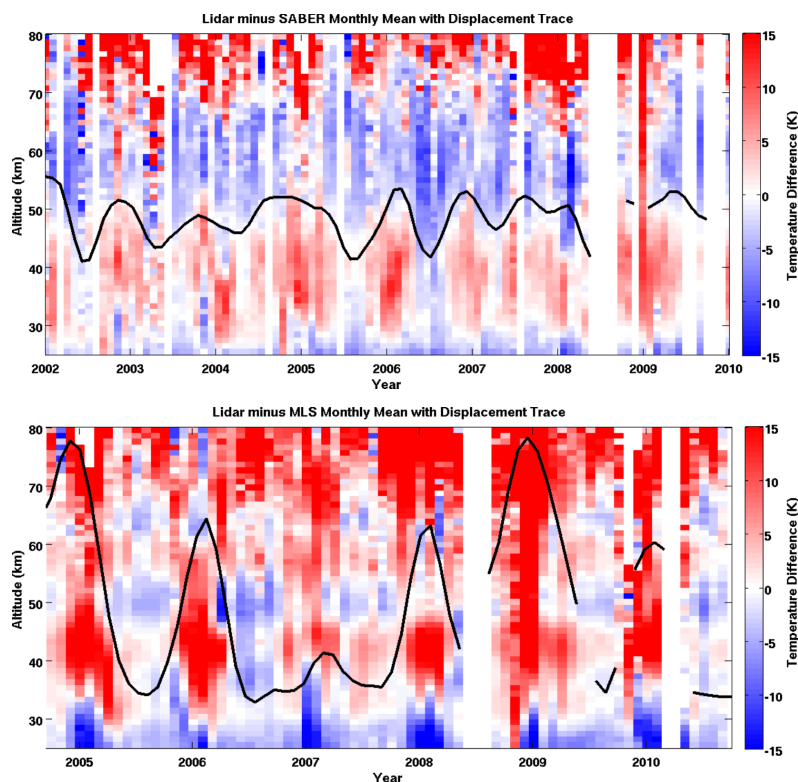


Figure 10: The upper panel features the monthly median temperature differences between the lidar and SABER with the estimated vertical displacement of the stratopause height overplotted. The lower panel features the monthly median temperature differences between the lidar and MLS with the estimated vertical displacement of the stratopause height overplotted.

6 Recalculated Lidar-Satellite Temperature Differences

We have attempted to make a more accurate comparison of the lidar and satellite temperatures by using the stratopause height as a common altitude reference. We re-calculated the lidar-satellite temperature differences shown in Fig. 3 and Fig. 5 after displacing the satellite measurement by a scalar value. Each satellite measurement was shifted vertically according to the lidar derived stratospheric displacements shown in Fig. 9.

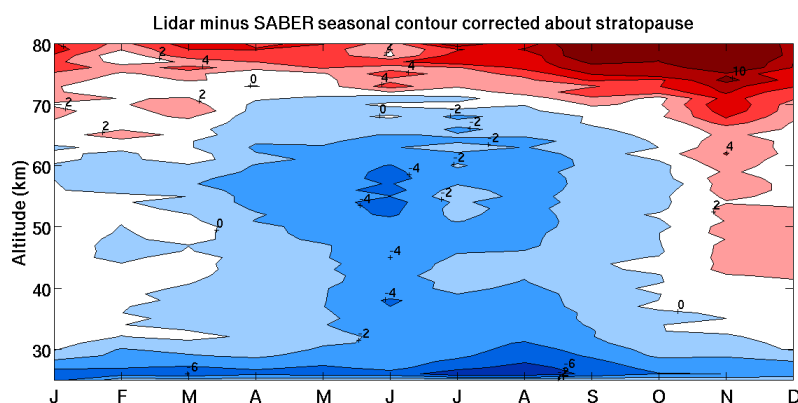


Figure 11: Corrected seasonal temperature differences between the lidar and the vertically displaced SABER temperatures. The maximum monthly average cold bias is reduced from -10 K in Fig. 3 to -4 K.

In Fig. 11 we see that by displacing the SABER temperature profiles so that the stratopause height is the same in both the lidar and satellite measurements we have eliminated the winter time stratospheric warm bias. The remaining summer time cold bias in both the stratosphere and mesosphere cannot be further minimized by a simple vertical shift. The altitude dependent correction required to correct the temperature lapse rate is beyond the scope of this work.

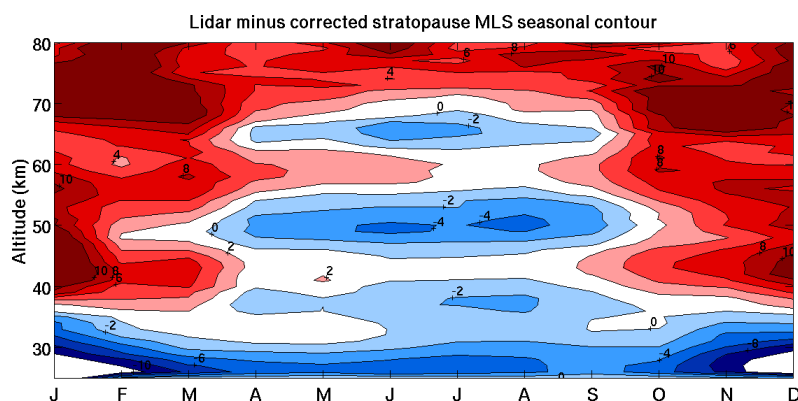


Figure 12: Corrected seasonal temperature differences between the lidar and the vertically displaced MLS temperatures. The structured nature of the temperature bias remains unchanged by the vertical correction.

In Fig. 12 we see that displacing the MLS temperature profiles was less successful than in the case of the SABER measurements. We have reduced the magnitude of beginning and end of winter time stratospheric warm bias by up to 4 K during the months of February, September, and October



240 but the correction does not completely eliminate the issue. As well we have an improvement of 2 K
 in the biased layer at 65 km. However, the horizontal layering inherent in the MLS temperature data
 makes determining a scalar correction even more challenging than in the case of SABER.

7 Discussion

7.1 The need for vertical altitude correction of satellite data

245 We have seen individual cases in Fig. 6 and Fig. 7 where both MLS and SABER temperature pro-
 files benefited from a slight vertical displacement based on lidar derived stratopause height. While
 this scalar adjustment does not correct for non-linear distortions in the altitude vector it can sig-
 nificantly reduce the magnitude of the temperature bias in the stratosphere and lower mesosphere.
 This technique does not seem to work well when the stratopause is highly disturbed as can be seen
 250 in the two winter time examples in Fig. 8. The implications of satellite underestimation of sudden
 stratospheric warming events is of particular concern to reanalysis projects attempting to model mid-
 dle atmosphere dynamics. However, by using lidar data to supplement the satellite record these fast
 dynamical processes can be better resolved.

7.2 Temperature biases between OHP lidar and SABER

255 In the companion publication (Wing et al., 2018a) we attempted to reduce the magnitude of the
 initialization induced lidar warm bias which is often reported above 70 km. We have reduced the
 bias by up to 5 K near 85 km and nearly 20 K at 90 km. There still remains some residual systematic
 warm bias between the lidar satellite comparisons in this publication. Further work needs to be done
 on the problem of lidar initialization to fully address the effects of noise and a priori choice on
 260 high altitude Rayleigh lidar retrievals. However, we cannot discount the possibility that some of the
 remaining temperature difference is due to incorrect altitudes in the satellite data product.

When considering the residual temperature differences between the OHP lidars and SABER after
 the altitude correction based on lidar derived stratopause height we can see that much of the seasonal
 variability in the stratosphere and mesosphere has been reduced. We are still left with a general
 265 summertime cold bias over most of the atmospheric column which now achieves a maximum of
 -4 K in the June mesosphere. We cannot explain this bias from the perspective of the lidar data as
 nothing in our range resolution changes, our data acquisition cadence and measurement duration
 are very similar (Wing et al., 2018a), and we are well into the linear region of lidar count rates
 and are not influenced by our a priori or saturated count rates. It is possible that there could be a
 270 tidal contribution as summertime lidar measurements start a bit later than wintertime measurements
 due to a shorter astronomical night. However, given that our criteria for coincidence were chosen to
 minimize the effects of the first few tidal harmonics this seems unlikely. It is also possible that there



is a seasonally dependent bias in the a priori used in the satellite retrieval of the geopotential height which could influence the satellite altitude vector.

275 The cold bias seen below 30 km is most likely due to possible contamination in the lidar data from aerosols and saturation in the low gain Rayleigh channel. Current OHP lidar measurements use Raman scatter data to correct for these effects and produce temperature profiles down to 5 km. However, this Raman data is not available for the entire 2002 to 2011 analysis period so we have opted not to include it in this work.

280 7.3 Temperature biases between OHP lidar and MLS

As with the comparison between the lidar and SABER, the lidar and MLS comparison has a pronounced warm bias above 70 km which is in keeping with previous studies. However, the magnitude and extent of this warm bias in MLS is much more pronounced than in the SABER comparison plot. Much of this difference is due to the reduced vertical resolution of MLS at these high altitudes.

285 The lidar MLS comparison has a wintertime stratospheric warm bias which is not much reduced by simply shifting the location of the MLS stratopause. It is almost universally the case that sudden stratospheric warmings seen by the lidar are missed or smoothed over in the corresponding MLS measurement. Figure 8 (upper panel) is very much a typical comparison for periods when the stratosphere is highly disturbed. The vertical structure which dominates much of the middle portion of the
290 lidar MLS comparison is difficult to account for. There is nothing in the lidar technique that could yield this pattern. The effect most likely comes from the averaging kernels in the satellite temperature retrieval. This is another perfect opportunity to incorporate lidar information into the satellite retrieval. Given the fixed width and amplitude of the vertical kernels in the lidar measurement, a lidar altitude and temperature vector could be used to recalculate the MLS kernels to eliminate these
295 structures.

7.4 Seasonality of Temperature biases between OHP lidar and satellites

We have seen the 5 K difference between lidar-SABER stratopause temperatures which was reported in (Sivakumar et al., 2011) however, unlike this study we have found a clear seasonal dependence. We have correlated this temperature bias directly to a vertical displacement of the satellite altitude
300 with respect to the lidar altitude and not with the Annual Oscillation. Further work must be done to explore the possibility of North Atlantic Oscillation/Annual Oscillation effects but a quick correlation of relative vertical displacement seen in Fig. 9 and a monthly average AO phase shows an R squared value of only 0.04 for SABER and 0.03 for MLS. There are isolated periods of up to a year where it seems like the correlations are significant however, it is clear that over a period of nearly
305 a decade the AO phase and winter time stratospheric temperature anomaly are not correlated. The 5 K stratospheric warm bias was attributed to tides in (Yue et al., 2014) however, this explanation



cannot explain the seasonal nature of this bias found in this work nor explain why a simple vertical displacement of the satellite stratopause height offers a suitable correction.

8 Conclusions

310 We can draw the following conclusions from the comparison of the lidar and satellite temperature measurements.

1) We have found the same systematic 5-15 K warm bias in the lidar-satellite comparisons above 70 km found in studies like (García-Comas et al., 2014), (Taori et al., 2011), (Taori et al., 2012), (Taori et al., 2012), (Dou et al., 2009), (Remsberg et al., 2008), (Yue et al., 2014), and (Sivakumar
315 et al., 2011). We have attempted to carefully account for the the background-induced warm bias in high altitude Rayleigh lidar temperatures. We believe that the algorithm set out in the companion publication (Wing et al., 2018a) is robust and accounts for many of the uncertainties in the lidar initialization process. However, we are as yet unable to determine to what extent the a priori estimate warms the lidar temperature retrieval at these heights.

320 2) We have seen a layered summer stratosphere-mesosphere cold bias in lidar-MLS seasonal temperature comparisons with peak differences at 37 km, 50 km, and 65 km. There is nothing in the lidar data or retrieval algorithm which could account for this structure.

3) The persistent summertime cold bias between the lidar and SABER results from a disagreement in the thermal lapse rate above and below the stratopause which is independent of the scalar
325 stratopause height offset. Given that lapse rate is a fundamental geophysical parameter further work must be done to explore possible errors in vertical resolution and altitude definition.

4) The periods of greatest lidar-satellite temperature disagreement are located during times when the middle atmosphere is highly disturbed. In particular, the amplitude of stratospheric warming events can be underestimated and features like double stratopauses can be missed in the satellite
330 measurements.

We have shown that ground based lidars can provide accurate and precise temperature measurements over decades. This kind of high vertical resolution temperature database is useful both as a validation source for other instruments as well as for fundamental geophysical research.

Acknowledgements. The data used in this publication were obtained as part of the Network for the Detection of
335 Atmospheric Composition Change (NDACC) and are publicly available (see <http://www.ndacc.org>, <http://cds-espri.ipsl.fr/NDACC>) as well as from the SABER (see <ftp://saber.gats-inc.com>) and MLS (see <https://mls.jpl.nasa.gov>) data centres for the public access via their websites. This work is supported by the project Atmospheric dynamics Research InfraStructure Project (ARISE 2) funded by funded by the European Union's Horizon 2020 research and innovation programme under grant agreement No. 653980 French NDACC activities are supported
340 by Institut National des Sciences de l'Univers/Centre National de la Recherche Scientifique (INSU/CNRS),



Université de Versailles Saint-Quentin-en-Yvelines (UVSQ), and Centre National d'Études Spatiales (CNES).

The authors would also like to thank the technicians at La Station Géophysique Gérard Mégie at OHP .



References

- Council, N. R.: Earth Science and Applications from Space: National Imperatives for the Next Decade and Beyond, The National Academies Press, Washington, DC, doi:10.17226/11820, <https://www.nap.edu/catalog/11820/earth-science-and-applications-from-space-national-imperatives-for-the>, 2007.
- data: Google, M.: Observatoire de Haute Provence (CNRS) Kernel Description, [https://www.google.fr/maps/place/Observatoire+de+Haute+Provence+\(CNRS\)/@43.9236737,5.7183398,2017](https://www.google.fr/maps/place/Observatoire+de+Haute+Provence+(CNRS)/@43.9236737,5.7183398,2017).
- Dou, X., Li, T., Xu, J., Liu, H.-L., Xue, X., Wang, S., Leblanc, T., McDermid, I. S., Hauchecorne, A., Keckhut, P., Bencherif, H., Heinselman, C., Steinbrecht, W., Mlynarczyk, M. G., and Russell, J. M.: Seasonal oscillations of middle atmosphere temperature observed by Rayleigh lidars and their comparisons with TIMED/SABER observations, *Journal of Geophysical Research: Atmospheres*, 114, n/a–n/a, doi:10.1029/2008JD011654, <http://dx.doi.org/10.1029/2008JD011654>, d20103, 2009.
- French, W. J. R. and Mulligan, F. J.: Stability of temperatures from TIMED/SABER v1.07 (2002–2009) and Aura/MLS v2.2 (2004–2009) compared with OH(6–2) temperatures observed at Davis Station, Antarctica, *Atmospheric Chemistry and Physics*, 10, 11 439–11 446, doi:10.5194/acp-10-11439-2010, <https://www.atmos-chem-phys.net/10/11439/2010/>, 2010.
- García-Comas, M., Funke, B., Gardini, A., López-Puertas, M., Jurado-Navarro, A., von Clarmann, T., Stiller, G., Kiefer, M., Boone, C. D., Leblanc, T., Marshall, B. T., Schwartz, M. J., and Sheese, P. E.: MIPAS temperature from the stratosphere to the lower thermosphere: Comparison of vM21 with ACE-FTS, MLS, OSIRIS, SABER, SOFIE and lidar measurements, *Atmospheric Measurement Techniques*, 7, 3633–3651, doi:10.5194/amt-7-3633-2014, <https://www.atmos-meas-tech.net/7/3633/2014/>, 2014.
- Hoppel, K. W., Baker, N. L., Coy, L., Eckermann, S. D., McCormack, J. P., Nedoluha, G. E., and Siskind, E.: Assimilation of stratospheric and mesospheric temperatures from MLS and SABER into a global NWP model, *Atmospheric Chemistry & Physics*, 8, 6103–6116, 2008.
- Johnson, K. W. and Gelman, M. E., eds.: Trends in upper stratospheric temperatures as observed by rocketsondes (1965–1983), vol. 18, 1985.
- Leblanc, T., McDermid, I. S., Hauchecorne, A., and Keckhut, P.: Evaluation of optimization of lidar temperature analysis algorithms using simulated data, *Journal of Geophysical Research: Atmospheres*, 103, 6177–6187, doi:10.1029/97JD03494, <https://agupubs.onlinelibrary.wiley.com/doi/abs/10.1029/97JD03494>, 1998.
- Meek, C. E., Manson, A. H., Hocking, W. K., and Drummond, J. R.: Eureka, 80° N, SKiYMET meteor radar temperatures compared with Aura MLS values, *Annales Geophysicae*, 31, 1267–1277, doi:10.5194/angeo-31-1267-2013, <https://www.ann-geophys.net/31/1267/2013/>, 2013.
- Mertens, C. J., Mlynarczyk, M. G., López-Puertas, M., Wintersteiner, P. P., Picard, R. H., Winick, J. R., Gordley, L. L., and Russell, J. M.: Retrieval of mesospheric and lower thermospheric kinetic temperature from measurements of CO₂ 15 μ m Earth Limb Emission under non-LTE conditions, *Geophysical Research Letters*, 28, 1391–1394, doi:10.1029/2000GL012189, <http://dx.doi.org/10.1029/2000GL012189>, 2001.
- Pautet, P.-D., Taylor, M. J., Pendleton, W. R., Zhao, Y., Yuan, T., Esplin, R., and McLain, D.: Advanced mesospheric temperature mapper for high-latitude airglow studies, *Appl. Opt.*, 53, 5934–5943, doi:10.1364/AO.53.005934, <http://ao.osa.org/abstract.cfm?URI=ao-53-26-5934>, 2014.
- Remsberg, E. E., Marshall, B. T., Garcia-Comas, M., Krueger, D., Lingenfelter, G. S., Martin-Torres, J., Mlynarczyk, M. G., Russell, J. M., Smith, A. K., Zhao, Y., Brown, C., Gordley, L. L., Lopez-Gonzalez, M. J.,



- Lopez-Puertas, M., She, C.-Y., Taylor, M. J., and Thompson, R. E.: Assessment of the quality of the Version 1.07 temperature-versus-pressure profiles of the middle atmosphere from TIMED/SABER, *Journal of Geophysical Research: Atmospheres*, 113, n/a–n/a, doi:10.1029/2008JD010013, <http://dx.doi.org/10.1029/2008JD010013>, d17101, 2008.
- Schwartz, M. J., Lambert, A., Manney, G. L., Read, W. G., Livesey, N. J., Froidevaux, L., Ao, C. O., Bernath, P. F., Boone, C. D., Cofield, R. E., Daffer, W. H., Drouin, B. J., Fetzer, E. J., Fuller, R. A., Jarnot, R. F., Jiang, J. H., Jiang, Y. B., Knosp, B. W., Krüger, K., Li, J. F., Mlynchak, M. G., Pawson, S., Russell, J. M., Santee, M. L., Snyder, W. V., Stek, P. C., Thurstans, R. P., Tompkins, A. M., Wagner, P. A., Walker, K. A., Waters, J. W., and Wu, D. L.: Validation of the Aura Microwave Limb Sounder temperature and geopotential height measurements, *Journal of Geophysical Research: Atmospheres* (1984–2012), 113, doi:10.1029/2007JD008783, <http://dx.doi.org/10.1029/2007JD008783>, 2008.
- Siva Kumar, V., Rao, P. B., and Krishnaiah, M.: Lidar measurements of stratosphere-mesosphere thermal structure at a low latitude: Comparison with satellite data and models, *Journal of Geophysical Research: Atmospheres*, 108, n/a–n/a, doi:10.1029/2002JD003029, <http://dx.doi.org/10.1029/2002JD003029>, 4342, 2003.
- Sivakumar, V., Prasanth, P. V., Kishore, P., Bencherif, H., and Keckhut, P.: Rayleigh LIDAR and satellite (HALOE, SABER, CHAMP and COSMIC) measurements of stratosphere-mesosphere temperature over a southern sub-tropical site, Reunion (20.8° S; 55.5° E): climatology and comparison study, *Annales Geophysicae*, 29, 649, <https://www.lib.uwo.ca/cgi-bin/ezpauthn.cgi?url=http://search.proquest.com/docview/869915562?accountid=15115>, 2011.
- Taori, A., Dashora, N., Raghunath, K., Russell, J. M., and Mlynchak, M. G.: Simultaneous mesosphere-thermosphere-ionosphere parameter measurements over Gadanki (13.5°N, 79.2°E): First results, *Journal of Geophysical Research: Space Physics*, 116, n/a–n/a, doi:10.1029/2010JA016154, <http://dx.doi.org/10.1029/2010JA016154>, a07308, 2011.
- Taori, A., Jayaraman, A., Raghunath, K., and Kamalakar, V.: A new method to derive middle atmospheric temperature profiles using a combination of Rayleigh lidar and O₂ airglow temperatures measurements, *Annales Geophysicae*, 30, 27–32, doi:10.5194/angeo-30-27-2012, 2012.
- Taori, A., Kamalakar, V., Raghunath, K., Rao, S., and Russell, J.: Simultaneous Rayleigh lidar and airglow measurements of middle atmospheric waves over low latitudes in India, *Journal of Atmospheric and Solar-Terrestrial Physics*, 78–79, 62–69, doi:10.1016/j.jastp.2011.06.012, 2012.
- Waters, J. W., Froidevaux, L., Harwood, R. S., Jarnot, R. F., Pickett, H. M., Read, W. G., Siegel, P. H., Cofield, R. E., Filipiak, M. J., Flower, D. A., Holden, J. R., Lau, G. K., Livesey, N. J., Manney, G. L., Pumphrey, H. C., Santee, M. L., Wu, D. L., Cuddy, D. T., Lay, R. R., Loo, M. S., Perun, V. S., Schwartz, M. J., Stek, P. C., Thurstans, R. P., Boyles, M. A., Chandra, K. M., Chavez, M. C., Chen, G.-S., Chudasama, B. V., Dodge, R., Fuller, R. A., Girard, M. A., Jiang, J. H., Jiang, Y., Knosp, B. W., LaBelle, R. C., Lam, J. C., Lee, K. A., Miller, D., Oswald, J. E., Patel, N. C., Pukala, D. M., Quintero, O., Scaff, D. M., Snyder, W. V., Tope, M. C., Wagner, P. A., and Walch, M. J.: The Earth observing system microwave limb sounder (EOS MLS) on the aura Satellite, *IEEE Transactions on Geoscience and Remote Sensing*, 44, 1075–1092, doi:10.1109/TGRS.2006.873771, 2006.
- Wing, R., Hauchecorne, A., Keckhut, P., Godin-Beekman, S., Khaykin, S., McCullough, E. M., Mariscal, J.-F., and d’Almeida, E.: Improved lidar measurements as a reference data set for the assessment of temperatures



- in the middle atmosphere: A) Systematic approach to lidar temperature retrievals and a 20 year comparison of two co-located French lidars, *Atmospheric Measurement Techniques*, Submitted, 2018a.
- 425 Wuebbles, D., Fahey, D., and Hibbard, K.: The Climate Science Special Report (CSSR) of the Fourth National Climate Assessment (NCA4), in: AGU Fall Meeting Abstracts, 2016.
- Xu, J., She, C. Y., Yuan, W., Mertens, C., Mlynarczyk, M., and Russell, J.: Comparison between the temperature measurements by TIMED/SABER and lidar in the midlatitude, *Journal of Geophysical Research: Space Physics*, 111, n/a–n/a, doi:10.1029/2005JA011439, <http://dx.doi.org/10.1029/2005JA011439>, a10S09, 2006.
- 430 Yuan, T., She, C.-Y., Krueger, D., Reising, S. C., Zhang, X., and Forbes, J.: A collaborative study on temperature diurnal tide in the midlatitude mesopause region (41N, 105W) with Na lidar and TIMED/SABER observations, *Journal of Atmospheric and Solar-Terrestrial Physics*, 72, 541–549, doi:10.1016/j.jastp.2010.02.007, 2010.
- Yue, C., Yang, G., Wang, J., Guan, S., Du, L., Cheng, X., and Yang, Y.: Lidar observations of the middle atmospheric thermal structure over north China and comparisons with TIMED/SABER, *Journal of Atmospheric and Solar-Terrestrial Physics*, 120, 80–87, doi:10.1016/j.jastp.2014.08.017, 2014.
- 435